FPCM-9 (2008)
The 9th International Conference on Flow Processes in Composite Materials
Montréal (Québec), Canada
8 ~ 10 July 2008

PREDICTION OF PERMEABILITY IN A DUAL-SCALE FIBER MAT USING TWO DIFFERENT UNIT CELLS

Hua Tan [1], Ehsan Mohseni Languri [1], Krishna M. Pillai [1, 2]

[1] *Department of Mechanical Engineering, University of Wisconsin-Milwaukee*
[2] *Corresponding author's Email: krishna@uwm.edu*

SUMMARY: Permeability is fundamental to an accurate simulation of mold-filling in liquid composite molding (LCM) technologies (such as RTM) that are used for manufacturing polymer composites. In this paper, unit cells representing the micro-structure of a biaxial stitched fiber mat are used by the 3D finite element based CFD simulation to estimate numerical permeability. Stokes and Brinkman equations are employed to model the saturated flow in the inter- and intra-tow regions, respectively, of the non-crimp fiber mat with a dual-scale pore structure. Two different unit cells are identified for the mat: one bigger and true to the mat architecture, and the other smaller but inaccurate, though including the essence of tow distribution. The experimental permeability of the mat is measured using the 1D flow experiment. A comparison of the numerical and experimental permeabilities reveals that the permeability estimated using the big (true) unit cell is less close to the real value as compared to the permeability estimated using the small (apparent) unit cell. Explanations such as nesting between the plies, tow deformation, and overlooking of stitches in the flow simulation, can be used to explain the larger error witnessed in the numerical permeability obtained from the geometrically accurate, big unit-cell. CFD simulation in the small unit cell is shown to be a quicker, less difficult, and paradoxically more accurate way of estimating the mat permeability.

KEYWORDS: Liquid Composite Molding (LCM), Resin Transfer Molding (RTM), unit cell, mold-filling, permeability

INTRODUCTION

Liquid Composite Molding (LCM) processes such as Resin Transfer Molding (RTM), vacuum assisted resin transfer molding (VARTM), and Seemann Composites Resin Infusion Molding Process (SCRIMP), are important methods for manufacturing polymer composites. Since LCM processes involve many processing parameters, numerical mold-filling simulations are essential for optimizing LCM mold designs and processing [1]. Darcy's law, which relates the volume-averaged resin velocity to the gradient of pore-averaged pressure, has been widely used to model the momentum transport phenomena of fluid flow through fibrous porous media in LCM [2-3]. For a successful simulation, the permeability of the fiber mats has to be accurately characterized so that the resin velocity in preforms, and hence the mold fill-time, can be accurately predicted. Various experimental measurement techniques have been developed to measure the permeabilities of fibrous media but most widely used are the 1-D flow and the radial flow based techniques [4-6]. In recent years, Computational Fluid Dynamics (CFD) has been found to be very useful in predicting the permeability of different kinds of fibrous preforms [7-8]. The accuracy of this method depends on the construction of a unit cell representing the meso-scopic structure of the fiber mats. In this study, two different unit cells are identified in the structure of a biaxial stitched fiber mat [9]. A simulation based on FEM is developed to solve the Stokes and Brinkman equations which model the saturated flow in the inter- and intra-tow regions of the unit cell, respectively. Based on the CFD simulation, the effective permeabilities along two main directions are estimated using Darcy's law.

GOVERNING EQUATIONS AND SIMULATION

For steady Stokes flows through the inter-tow region, the fluid motion is governed by the continuity and Stokes equations, which are expressed in vector form as

$$\nabla \cdot \mathbf{u} = 0 \quad (1) \quad \text{and} \quad \nabla p = \mu \nabla^2 \mathbf{u} \quad (2)$$

where $\mathbf{u}$ is velocity, p is pressure, and μ is fluid viscosity. ∇ is the gradient operator. The Brinkman equation can be used to model the flow through the intra-tow region of the unit cell. The Brinkman equation is actually the volume averaged momentum balance equation that can be described as

$$-\nabla \langle p \rangle^f + \mu' \nabla^2 \langle \mathbf{u} \rangle - \mu \mathbf{K}^{-1} \langle \mathbf{u} \rangle = 0 \qquad (3)$$

where $\langle \mathbf{u} \rangle$ is the volume averaged velocity, $\langle p \rangle^f$ is the pore average pressure, $\mathbf{K}$ is the permeability tensor of the tow, and μ' represents the effective viscosity. The longitudinal (along the fibers) and transverse (across the fibers) permeabilities of the fiber tow are estimated using the equations proposed by Gebart [10].

A 3D finite element code is developed to simulate the steady flow through the inter-tow gaps and porous tows within a unit cell. The mixed finite element model and consistent penalty method are used to solve the governing equations [12]. The velocity and pressure are primitive variables in our FE formulation. The eight-node isoparametric trilinear element Q_1Q_0 with a piecewise constant discontinuous pressure approximation is used in the simulation [12]. One important issue involved in the simulation of flow through the tow and gap interface is the boundary conditions (b.c.) at this interface between the clear-fluid and porous regions. Our other study [11] shows that for the low or moderate porosities found in fiber tows, the most commonly considered Beaver & Joseph slip-velocity b.c., the stress-continuity b.c., and Whitaker's stress-jump b.c. lead to almost identical results. So for the simplicity of FE formulation, the velocity and stress are assumed to be continuous at the tow-gap interface in this study.

UNIT CELLS

In the present study, permeability of a biaxial stitched mat from Owens Corning is measured using the 1D flow experiment. The biaxial mat has two layers of stitched fiber tows oriented in mutually perpendicular directions (Fig. 1A). Some unique structural characteristic of this type of biaxial mat is as follows. In both the *z* and *x* directions (henceforth *z* and *x* directions are referred to as 0^0 and 90^0, respectively), one can identify clusters consisting of five parallel tows each, while the clusters themselves are separated by thinner tows, running in the middle of meso-scopic gaps. Therefore, a repeated unit cell marked as a red square in Fig. 1A, and with five tows in each direction, can be easily identified. Another smaller unit, which can recreate the unit cell by repeating, can be identified within the unit cell as well. Unlike the previous unit cell, there is only one tow in both directions in this smaller 'unit cell'. In order to distinguish between the two unit cells, we refer the former as the big (true) unit cell and the latter as the small (apparent) unit cells. The geometrical representation of tows in the big unit cell is shown in Fig. 1B.

The finite element models of the big and small unit cells are shown in Fig. 2 and Fig. 3. The sizes of the big and small unit cells are 2.16 cm × 2.07 cm × 0.0787 cm and 0.391 cm × 0.382 cm × 0.0787 cm, respectively. The FE model of the big unit cell contains 125,952 nodes and 114,000 hexahedron elements, whereas the small unit cell has 4,921 nodes and 4,032 elements. Since the distance between tows within a cluster of five tows is smaller than that between the clusters, which means that the gap region of the big unit cell is larger than that of the small unit cell, we expect the numerical permeability predicted using the big unit cell to be higher than that using the small unit cell. However, though the small unit-cell FE model does not reflect the structure of biaxial mats accurately, it does contain much less number of nodes and elements than the big unit cell, which means it can give us a much quicker estimation of permeability of the biaxial fiber mat.

Computed from the permeability model proposed by Gebart [10], the longitudinal and transverse permeabilities of the tows oriented in the 0^0 direction are 1.23×10^{-9} cm^2 and 2.48×10^{-10} cm^2, respectively. The longitudinal and transverse permeabilities of the tows oriented in the 90^0 direction are 1.8×10^{-8} cm^2 and 3.73×10^{-9} cm^2, respectively. (The porosity of tows along the 0^0 and 90^0 directions is estimated as 0.2 and 0.15, respectively. We assume the fibers within the tows to be arranged in a periodic hexagonal form. The fiber diameter is 15 µm.) The pressure b.c. of 100 Pa and 0 Pa are applied on two mutually opposite surfaces of a unit cell along the flow direction to drive the 0^0 or 90^0 direction flows. Symmetric b.c.s are imposed on the remaining surfaces of unit cell. Then the effective permeability along 0^0 or 90^0 directions can be calculated by using in Darcy's law the average velocity through the unit cell and the applied pressure gradient.

RESULTS, DISCUSSION AND CONCLUSION

For the big unit cell, the pressure and velocity contours for 0^0 and 90^0 flows are shown in Fig. 4 and 5, respectively. For the small unit cell, the pressure and velocity contours for 0^0 flows are shown in Fig. 6. Based on these flow simulations within the two unit cells, the effective permeabilities along the 0^0 and 90^0 directions estimated using Darcy's law are listed in Table 1.

As expected, the permeability estimated using the small unit cell is smaller than the one obtained from the big unit cell because of the larger gaps in the latter. Moreover the numerical permeabilities obtained from both the small as well as big unit cells are close to the experimental results. Since flow simulation with the small unit cell can result in a significant saving of computational time, the choice of using the small unit cell is appropriate despite its less accurate representation of the mat architecture.

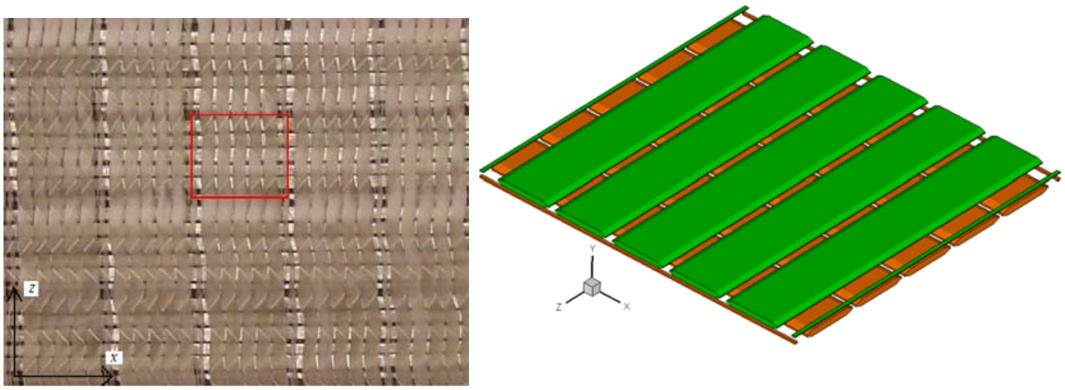

Fig. 1 (A) A photo of the biaxial fiber mat. (B) The big unit cell showing the two fiber-tow directions.

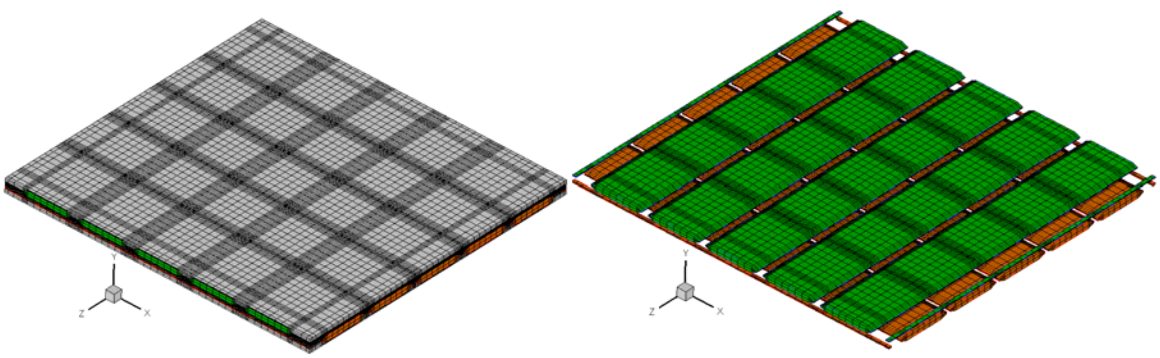

Fig. 2 Finite element mesh for the big (true) unit cell: (A) the whole unit cell; (B) just the fiber tows.

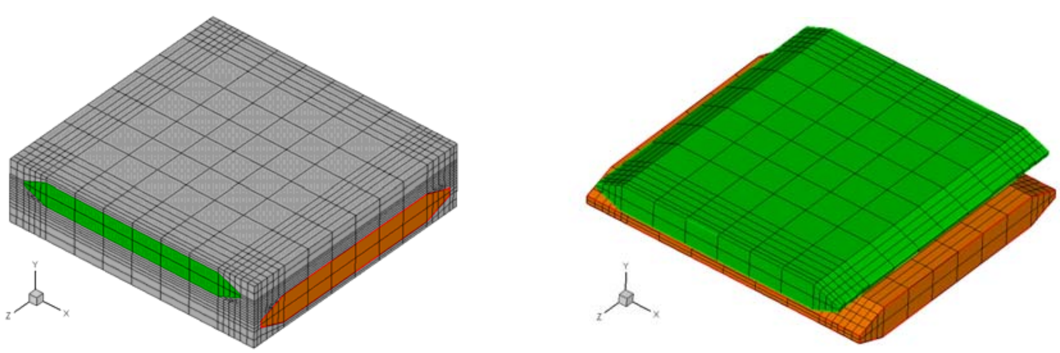

Fig. 3 Finite element mesh for the small (apparent) unit cell: (A) the whole unit cell; (B) just the fiber tows.

It is also clear from Table 1 that the numerical permeabilities obtained from the big unit cell are higher than the experimental permeabilities. We think there can be several explanations. First, the nesting of fiber mats in an LCM mold is very common. So the nesting in a stack of the biaxial fiber mats during the 1D flow experiment decreases the cross-section of meso-scale flow channels between tow clusters, thereby reducing the big unit-cell permeability. Second, the fiber mats are not rigid and often deform during packing or under the fluid pressure. The deformation of fiber mats changes the channels, which definitely has a bearing on the mat permeability. Lastly, there are threads stitching the fiber tows together in the biaxial mat. We ignored them while

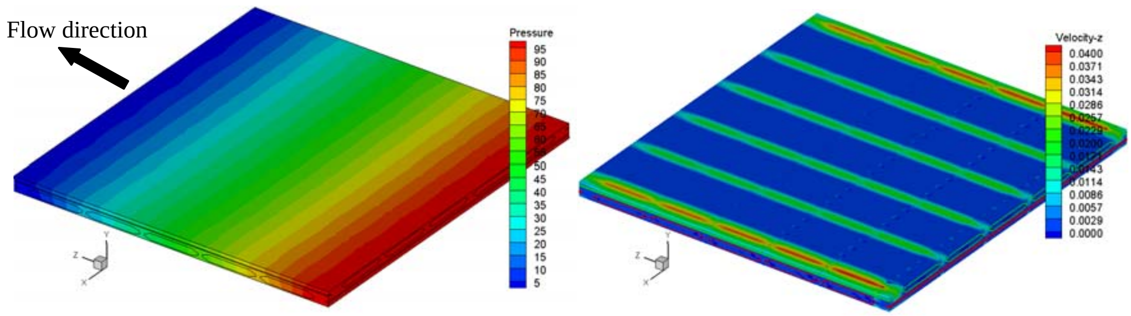

Fig. 4 Flow along the 0^0 direction of the big unit cell: (A) pressure contours; (B) velocity contours.

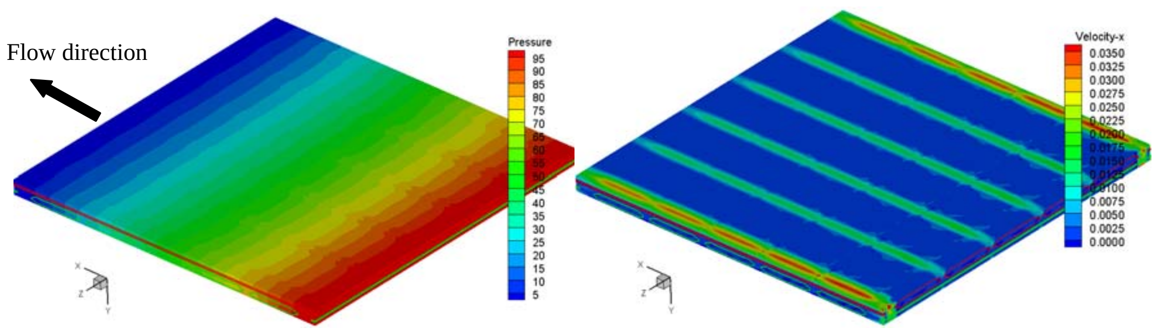

Fig. 5 Flow along the 90^0 direction of the big unit cell: (A) pressure contours; (B) velocity contours.

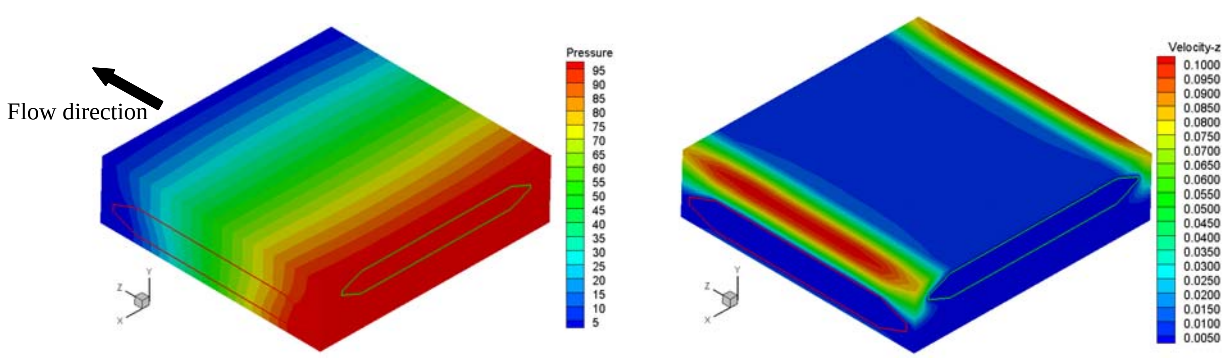

Fig. 6 Flow along the 0^0 direction of the small unit cell: (A) pressure contours; (B) velocity contours.

constructing the unit cell FE models. These impermeable threads create narrow ‘throats’ in the inter-tow channels and thus decrease the permeability of fiber mats. Although these factors complicate the permeability prediction using unit cells, we feel it is still one of the most effective and accurate approach in predicting the permeability of fiber mats.

Table 1 Comparison of the numerical and experimental permeabilities of the biaxial stitched mat

	K_0^0 ($\times 10^{-9}$ m^2)	K_{90}^0($\times 10^{-9}$ m^2)
Small unit cell	1.786	1.279
Big unit cell	3.037	2.514
Experimental	2.036	1.615

ACKNOWLEDGMENTS

We would like to thank the National Science Foundation (USA) for providing funding to conduct this research through its CAREER research grant. Material help from Owens-Corning Inc. in the form of fiber mats is also gratefully acknowledged.

REFERENCES

1. Advani, S.G. (editor): “Flow and Rheology in Polymer Composites Manufacturing, Chapter: Governing Equations for Resin Transfer Molding”, *Elsevier*, Amsterdam, 1994.

2. C.A. Fracchia, J. Castro and C.L. TuckerIII, “A Finite Element/Control Volume Simulation of Resin Transfers Molding”, In *Proceedings of the American Society for Composites, Fourth Technical Conference*, Lancaster, PA, Technomic, p. 157-166.

3. Richard S. Parnas and Andrew J. Salem. “A Comparison of the Unidirectional and Radial In-plane Flow of Fluids through Woven Composite Reinforcements”, *Polymer Composites*, 14(5): 383-394, 1993.

4. B.R. Gebart and P. Lindstrom, “Measurements of In-plane Permeability of Anisotropic Fiber Reinforcements”, *Polymer Composites*, v 17, 43-51, 1996.

5. C. Lekakou, M.A.K. Johari, D. Norman, and M.G. Bader, “Measurement Techniques and Effects on In-plane Permeability of Woven Clothes in Resin Transfer Molding”, *Composites: Part A*, 27A, 401-408, 1996.

6. V.H. Hammond and A.C. Loos, “The Effects of Fluid Type and Viscosity on the Steady-state and Advancing Front Permeability Behavior of Textile Performs”, *Journal of Reinforced Plastics and Composites*, v 16, n1, 50-72, 1997.

7. Ngo, N.D. and Tamma, K.K., "Micro-Scale Permeability Predictions of Porous Fibrous Media", *International Journal of Heat and Mass Transfer*, 44, 3135-3145, 2001.

8. Nordlund M. and Lundstrom T.S., "Numerical Study of the Local Permeability of Non Crimp Fabrics", *Journal of Composite Materials*, 39, 929-947, 2005.

9. Hua Tan, Tonmoy Roy and Krishna. M. Pillai, "Variations in Unsaturated Flow with Flow Direction in Resin Transfer Molding: An Experimental Investigation", *Composites: Part A*, 38, 1872-1892, 2007.

10. Gebart, B.R., "Permeability of Unidirectional Reinforcements for RTM", *Journal of Composite Materials*, 26, 1100-1133, 1992.

11. Hua Tan, Xiaomin Chen, Krishna M. Pillai, T.D. Papathanasiou, "Boundary Conditions at Interface between the Clear-Fluid and Porous Medium Domains", *FPCM-9*, Montreal, July 8-10, 2008.

12. J. N. Reddy, "Penalty Finite Element Analysis of 3D Navier-Stokes Equations", *Comput. Meth. Appl. Mech. Eng.*, 35, 87-106 (1982).